Research Square

Preprints are preliminary reports that have not undergone peer review.
They should not be considered conclusive, used to inform clinical practice,
or referenced by the media as validated information.

CFD-researches of centrifugal compressor stage vane diffusers

Aleksey Borovkov
Peter the Great St.Petersburg Polytechnic University
Yuri Galerkin
Peter the Great St.Petersburg Polytechnic University
Evgeniy Petukhov
Peter the Great St.Petersburg Polytechnic University
Aleksandr Drozdov
Peter the Great St.Petersburg Polytechnic University
Vladimir Yadikin
Peter the Great St.Petersburg Polytechnic University
Aleksey Rekstin
Peter the Great St.Petersburg Polytechnic University
Vasiliy Semenovskiy
Peter the Great St.Petersburg Polytechnic University
Olga Solovyeva
Peter the Great St.Petersburg Polytechnic University
Lyubov Marenina (marenina_ln@mail.ru)
Peter the Great St.Petersburg Polytechnic University

Research Article

Keywords: centrifugal compressor, vane diffuser, CFD simulation, loss coefficient, efficiency

Posted Date: March 19th, 2021

DOI: https://doi.org/10.21203/rs.3.rs-248189/v1

License: This work is licensed under a Creative Commons Attribution 4.0 International License.
Read Full License

CFD-RESEARCHES OF CENTRIFUGAL COMPRESSOR STAGE VANE DIFFUSERS

Aleksey Borovkov, Yuri Galerkin, Evgeniy Petukhov, Aleksandr Drozdov, Vladimir Yadikin, Aleksey Rekstin, Vasiliy Semenovskiy, Olga Solovyeva, Lyubov Marenina*

Peter the Great St.Petersburg Polytechnic University, St.Petersburg, Russia
*corresponding author: marenina_ln@mail.ru

ABSTRACT

The paper presents result of CFD simulations of a series of centrifugal compressor stage vane diffusers in the Ansys CFX. Objects of research are vane diffusers with external relative diameter (relative to the diameter of the impeller) equal to 1.5, vane inlet angle of 20 degrees, relative vane heights of 0.025, 0.034, 0.045, 0.06, 0.08, vane profile curvature angles of 10, 15, 20 degrees. The characteristics of polytrophic efficiency, loss coefficient, recovery coefficient, ratio of inlet and outlet velocities, flow deviation angle versus incidence angle are set. The analysis of the flow structure in the vane diffuser channels is presented. Unlike with a straight vane cascade, the deviation angle in the circular rows of vane diffusers tends to increase with increasing row density. This may be due to the complex nature of the interaction of the active part of the flow with separation zones. In rows with almost straight vanes at a lower density, the separation zone on the pressure side decreases, and even shifts to the very end of the suction side.

Keywords: centrifugal compressor, vane diffuser, CFD simulation, loss coefficient, efficiency

b	blade height, channel width in the direction of rotor axis;
c	absolute flow velocity;
c_p	specific heat capacity at constant pressure;
c_u	tangential component of absolute velocity;
D	diameter;
h_p	polytrophic pressure;
h_d	dynamic pressure;
h_l	lost pressure in stage flow path;
i	incidence angle;
k	isentropic coefficient;
l	blade length;
$\bar{m}$	mass flow rate;
M	Mach number, force moment;
p	pressure;
r	radius;
R	gas constant, curvature radius;
Re	Reynolds number;
t	distance between the vanes;
T	temperature;
z	number of vanes;
α	angle between absolute velocity and circumferential direction;
α_v	angle between blade midline tangent and circumferential direction;
δ_v	blade thickness;
ζ	loss coefficient;
η	polytrophic efficiency;
θ	profile curvature angle, degree;
ν	kinematic viscosity;
ξ	recovery coefficient;
ρ	gas density;

1. INTRODUCTION

Improvement of gas-dynamic design of centrifugal compressors is one of the areas of activity of the "Gas dynamics of turbomachines" laboratory. In some cases, CFD simulations are not that efficient in calculation of centrifugal compressors and centrifugal stages characteristics [1-3,23,34]. Mathematical modeling techniques are widely used in engineering practice [12-13,18,22,28-30]. The contribution of the Polytechnic University (SPbPU) scientific school is the creation of the Universal modeling method [7-9,18,24-26,33]. The main problem of modeling lies in the calculation of the compressor stage efficiency. Pressure losses are calculated separately by the place of origin and physical nature and then are summed.

In the recent versions of the Method the head losses in impellers, diffusers, return channels and scrolls were calculated using appropriate mathematical models – systems of algebraic equations with determining gas dynamic parameters and empirical coefficients [8]. Researches [4-6,14] have shown that CFD methods are quite efficient for simulation of the stage stator elements. Approximation of the vaneless diffuser (VLD) characteristics calculated by CFD methods [5-6,19,27,31] is used as a mathematical model of this element in the 8th version of the Universal modeling method [10]. The same results were taken as a basis for the choice of vaneless diffuser sizes in the programs of preliminary design of the Universal Modeling Method [16,32].

The purpose of the CFD research of vane diffusers (VD) is the same as with the classic approach: to examine the characteristics of diffusers in a wide range of design parameters, to approximate their characteristics for the calculation of a diffuser in the mathematical model of the centrifugal stage and to approximate the optimal size of

diffusers for the mathematical model of the preliminary design. The present research is the first stage in which diffusers with only a relative diameter $\bar{D}_4 = 1.50$ and the vane inlet angles $\alpha_{v3} = 20°$ were researched. Along with the results of simulations of diffusers with other values of diameters and vane inlet angles, these results will be used in mathematical models and design recommendations. Unexpected was the structure of the flow in the diffuser with different vane angles of curvature and the influence of the number of vanes on the deviation angle. The problem is analyzed in the proper sections of the text and in the 3.4 Discussion in particular.

2. OBJECTS AND METHODS

2.1 Methodology description

The theory of axial turbomachines is largely based on the results of experiments exposing a vane cascade to air flow in wind tunnels. Measurement of parameters in front of the row and after the row is performed at some distance in sections where the flow parameters are almost the same. At the inlet, the flow is potential, the total pressure of the gas particles is the same. The inlet section is selected at a distance where the effect of the step unevenness of the flow in the row on the incoming flow is sufficiently weakened. At the outlet, a mixing process is added to the step unevenness – the equalization of the total pressure. The measuring section should be located at a greater distance.

In a virtual wind tunnel, measurements of the flow parameters that determine the characteristics of the row must also be carried out in sections with a uniform flow. When testing the circular row of vane diffuser there is a problem. The vaneless spaces in front of the row and behind the row act as diffusers where flow parameters change as opposed to the row of axial turbomachines. The question of the simulations method of vane diffusers was researched in detail by the authors earlier. The object of research is shown in figure 1.

The object of research is located between cross sections "2" and "4". Actually, the vane row of the diffuser is limited by cross sections "3" and "4". Vaneless space – section "2-3" – is also included in the test object. According to the results of previous researches, the flow is fairly uniform in cross section $\bar{D}_1 = 0.80$ $(D_1/D_3 = 0.727)$ and in cross section $\bar{D}_5 = 2.50$ $(D_5/D_4 = 1.667)$.

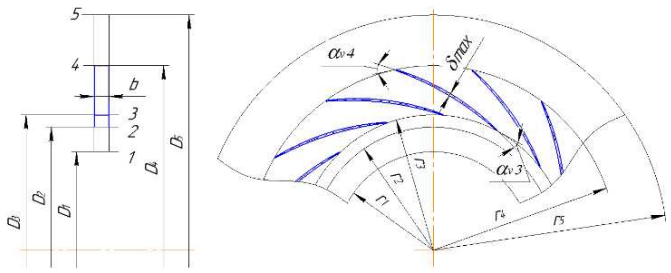

FIGURE 1: VANE DIFFUSER IN VIRTUAL WIND TUNNEL

To obtain sufficient information for the mathematical modeling of characteristics and recommendations for the preliminary design, it is necessary to research the influence of all parameters that determine the shape of the flow path, the scalar quantities of compressibility (M, k) and viscosity (Re), the operating mode (flow inlet angle, incidence angle).

Geometric parameters of the VD flow path:

- relative diameter of the vane leading edge $\bar{D}_3$. In his classical works, V.F. Ris [17] recommended values for $\bar{D}_3 = 1.10 - 1.15$. There are indications that the reduction of $\bar{D}_3$ increases efficiency, but the risk of breakdowns due to periodic unsteadiness of nz (rpm × vane number) increases too. However, in [20] there is information about the flow path of the 16 MW compressor unit of the CC 248-76-1,72 type with a reduced value $\bar{D}_3 = 1.05$ (discharge pressure 7.5 MPa). Designed by Universal modeling method, these flow paths have been produced for 20 years and operated successfully. In the presented paper, the tested value $\bar{D}_3 = 1.10$, recommended after [17] in the Universal modeling method [16,32];
- relative diameter of the vane trailing edge $\bar{D}_4$; value 1.50 is considered;
- the relative vane height $\bar{b}_3$; values 0.025, 0.034, 0.045, 0.06, 0.08 are considered;
- vane inlet angle α_{v3}; value 20° is considered;
- vane outlet angle α_{v4} or the profile curvature angle $\Delta\alpha_v = \alpha_{v4} - \alpha_{v3}$; values of $\Delta\alpha_v$ 10, 15, 20 degrees are considered. In [8] the principal influence of positive (center of curvature from the suctions surface) curvature and negative (center of curvature from the pressure surface) curvature of the profile is indicated. The boundary value of the curvature angle is a straight blade with a radius of curvature $R_v = \infty$ at $\alpha_{v4\,s.v.} = \arccos\left(\cos\alpha_{v3}\frac{D_3}{D_4}\right)$. For $\alpha_{v3} = 20°$ vanes are straight at $\alpha_{v3\,s.v.} = 46.40°$. At a maximum curvature angle of 20 degrees, the diffuser vanes have a slightly convex pressure surface and a concave, almost straight suction surface;
- number of vanes z_{VD}. The bulk of the simulations are carried out for three values of the vanes number, varying near row density $l/t \approx 1.7–2.1$ recommended in [17]. For some variants, simulations are carried out for the range of 10-26 vanes;
- the shape of the vane middle line. According to the recommendations [8,18], the middle line of the vanes is the circular arc. This form provides a uniform load distribution and a favorable velocity diagram;
- vane profile. Frequently used wing profiles are logically used in straight rows of axial compressors. In the circular rows of the centrifugal compressors they should be used in conformal transformation. Calculations in [14] showed that the two-arc profiles, as in figure 1, are slightly better than the wing profiles. In the proposed work, the vanes have a two-arc profile with a maximum thickness $\bar{\delta}_{max} =$ 3.4 mm;

According to previous research and developed recommendations [15], the Ansys CFX software package was used for simulations. Second-order schemes were used for discretization. At the inlet were varying the inlet flow angle (incidence angle) and set $p_1^* = 1\ atm$ and $T_1^* = 288\ K$; at the outlet we set the mass flow rate corresponding to the flow rate in cross section "2" at $M = 0.5$ (170.5 m/s); Reynolds number range $Re_{b2} = \frac{C_2 b_2}{\nu_1} = 102000..327000$.

Due to wide ranges of parameters being considered computational costs for case should be moderate. For channel mesh topology O4H was selected. It is composed by O block for blade and four H blocks for: upstream, downstream, up and down to the vane section. Total number of elements is 257536 with maximum expansion ratio 2.2, aspect ratio 740 (for boundary layer elements), minimal skewness 34. Mesh sensitivity analysis was carried out for one vane channel, refined mesh for one channel (800k elements) and 15 channels with regular mesh. Analysis showed close results so regular mesh for one channel was used for further simulations. Also the results for k-ε and k-ω SST turbulence models was compared. For boundary values of incidence angle k-ε showed almost no flow separation. Such simulation was held for plain diffuser with separating flow regime and gave same difference in flow pattern. For SST model curvature correction additionally used to avoid detachment over- prediction.

The results obtained with ANSYS CFX are used to analyze the flow structure and calculate the characteristics of the VD. In purely applied terms, the characteristics are needed to calculate the flow parameters at the outlet of the VD. In [8] it is shown that to solve the problem it is enough to know only two coefficients characterizing the operation of the diffuser, for example, efficiency and loss coefficient. But to understand the working process, the authors calculated the characteristics of the following dimensionless parameters of the VD and gave the following coefficients characterizing the operation of the diffuser depending on the incidence angle:

- polytrophic efficiency $\eta = \frac{h_p}{-h_d} = \frac{\ln(p_4/p_2)}{\frac{k}{k-1}\ln(T_4/T_2)}$;
- loss coefficient $\zeta = \frac{h_w}{0.5c_2^2} = (1-\eta)\left(1-\frac{c_4^2}{c_2^2}\right)$;
- recovery coefficient $\xi = \frac{h_p}{0.5c_2^2} = 1 - \frac{c_4^2}{c_2^2} - \zeta$;
- velocity ratio (flow deceleration) c_4/c_2;
- flow deviation angle at the VD exit $\Delta\alpha = \alpha_{v4} - \alpha_3$.

At diffusers' exit separation zone exists. It dissipates at some distance due to mixing process. Total pressure and other parameters must be measured at some distance when flow becomes quasi uniform. Analysis of the flow parameters calculated and averaged in cross section "4" showed that their values do not reflect the actual workflow. For example, the deviation angle had large negative values. This contradicts the indisputably correct row theory and is not confirmed by the flow pattern – calculated flow paths. The problem and exit cross section position is explained in [15].

The flow parameters are averaged by energy and taken at cross section "5" where the mixing process of low-energy and high-energy particles is completed, and the flow is almost uniform. Since in the vaneless space wall boundaries between the cross sections "4" and "5" are set to free slip (smooth walls without adhesion conditions) and the flow is practically incompressible, it is correct to calculate the flow parameters in the following way:

- outlet VD velocity $c_4 = \frac{c_5}{D_4/D_5}$;
- outlet flow angle $\alpha_4 = \alpha_5$;
- temperature $T_4 = T_{inl}^* - \frac{c_4^2}{2c_p}$;
- temperature $T_5 = T_{inl}^* - \frac{c_5^2}{2c_p}$;
- static pressure at the VD outlet $p_4 = p_5/(T_5/T_4)^{3.5}$.

2.2 Geometric and gas-dynamic parameters of VD affecting the flow pattern

For any diffuser the main factor determining the flow structure is the cross-section area *f* ratio. For VD: $\frac{f_4}{f_3} = \frac{\sin\alpha_{v4}}{\sin\alpha_{v3}}\frac{D_4}{D_3}$ (subscripts are shown in fig. 1).

For well-studied straight-axis diffusers [11] the second main factor is the cone angle. For flat diffusers it is the angle between its walls. By analogy for VD it is the opening angle $\nu_{VD} = 360°/z$.

In vane rows instead of the cone angle a relative step or the mutual value—the row density is usually used [18]:

$$\frac{l}{t} = \frac{z\lg(D_4/D_3)}{2.73\sin\frac{\alpha_{v3}+\alpha_{v4}}{2}} \quad (1)$$

In practice, for calculations the similar formula is used:

$$\frac{l}{t} = \frac{z\left(\frac{\bar{D}_4}{\bar{D}_3}-1\right)}{\pi\left(\frac{\bar{D}_4}{\bar{D}_3}+1\right)\sin\frac{\alpha_{v3}+\alpha_{v4}}{2}} \quad (1A)$$

Since the vane middle line has the shape of a circular arc, it can be calculated exactly according to the scheme in figure 2.

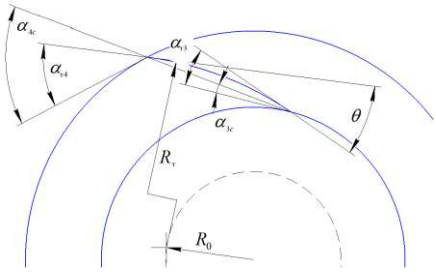

FIGURE 2: CALCULATION OF THE LENGTH OF THE ARC BLADE

Radius of the arc of the vane middle line:

$$R_v = \frac{r_4^2 - r_3^2}{2(r_4\cos\alpha_{v4} - r_3\cos\alpha_{v3})},$$

$$\bar{R}_v = \frac{\bar{D}_4^2 - \bar{D}_3^2}{4(\bar{D}_4 \cos\alpha_{v4} - \bar{D}_3 \cos\alpha_{v3})} \quad (2)$$

The chord of the arc is determined by angles:

$$\alpha_{3c} = \alpha_{v3} - 0.5\theta,\ \alpha_{4c} = \alpha_{v4} + 0.5\theta \quad (3)$$

Chord angle on diameter D_4 is equal to straight vane outlet angle:

$$\cos\alpha_{4c} = \frac{r_3}{r_4}\cos\alpha_{3c} \quad (4)$$

The equation for calculating the central angle of the vane arc is solved by substitution:

$$\cos(\alpha_{v4} - 0.5\theta) = \frac{r_3}{r_4}\cos(\alpha_{v3} - 0.5\theta) \quad (5)$$

The length of the vane:

$$\bar{l} = 2\pi\bar{R}_v \frac{\theta_v}{360^\circ} \quad (6)$$

Average relative pitch:

$$\bar{t} = \frac{\pi}{2z}\left(\bar{D}_4 + \bar{D}_3\right) \quad (7)$$

The density of the row:

$$\frac{l}{t} = z\frac{4\bar{R}_v}{\bar{D}_4 + \bar{D}_3}\frac{\theta_v}{360^\circ} \quad (8)$$

The calculations showed that compared to the more accurate formula (8), the row density according to the formula (1A) is greater by 1.5– 2%, according to the formula (1) – by 3 – 5%. The l/t values below are calculated using the formula (1A).

In the Universal modeling method, the advantage is given to gas-dynamic parameters. The concept of the average aerodynamic load is used to select the number of the impeller blades [8]. With regard to the vane diffuser, the problem is formulated as follows.

The change in the momentum due to the impact of the vanes:

$$dM_z = d(c_u r\bar{m}) \quad (9)$$

$$dM_z = z \cdot \Delta p \cdot dr \cdot r = z \cdot \rho \cdot \Delta c \cdot c \cdot dr \cdot r \quad (10)$$

$$\bar{m} = \rho \cdot 2\pi r \cdot c \cdot \sin\alpha \quad (11)$$

$$\frac{2\pi}{z}(c_{u3}r_3 - c_{u4}r_4) = \int_{r_3}^{r_4} \Delta c \cdot dl \quad (12)$$

Taking $\Delta c = \Delta c_{av}$ and examining the diffuser together with the vaneless section ($c_{u3}r_3 \approx c_{u2}r_2$):

$$\Delta\tilde{c}_{av} = \frac{\Delta c_{av}}{c_2} = \frac{\pi}{z}\frac{\cos\alpha_3 - \bar{D}_4\frac{c_4}{c_2}\cos\alpha_4}{\bar{l}} \quad (13)$$

In contrast to the geometric parameter l/t, the average load more comprehensively reflects the essence of the workflow. By inducing a rearrangement of the flow at the row inlet, the load affects the actual incidence angle and the flow deviation [8] at the row outlet. The vane load varies depending on the inlet flow angle. Its change helps to analyze the change of flow parameters in the VD and choose the optimal VD sizes.

3. RESULTS AND DISCUSSION

3.1 Flow structure features

The deceleration of the flow in the VD is very significant. The velocity decreases approximately by three times according to the continuity equation:

$$\frac{c_4}{c_3} = \frac{\rho_3}{\rho_4}\frac{D_3}{D_4}\frac{\sin\alpha_3}{\sin\alpha_4} \quad (14)$$

Therefore, unlike the blade rows of axial compressors, flow separation is inevitable even with a non-incidence inlet. Visualization of the separation zone in the VD in the design mode by introducing a powder dye into the flow is shown in figure 3.

FIGURE 3: EXPERIMENTAL VISUALIZATION OF THE SEPARATION ZONE IN VD FROM [18]

Unlike with a vane cascade, the convex surface of the vane is a pressure surface where the flow rates are less than on the opposite concave side. The velocity at the flow separation point is less than the average velocity and the kinetic energy in the separation zone is small. Therefore, the presence of separation does not prevent a fairly high efficiency of the vane diffusers.

Figures 4 - 6 demonstrate flow separation intensiveness in different diffusers at different incidences. Shown below at mid span separation zones are of the same character as visualized ones on a diffuser wall in figure 3. Figure 4 shows the gas flow structure in the vane diffuser with $\bar{b}_3 = 0.045, \alpha_{v3} = 20^\circ, \alpha_{v4}30^\circ, z = 17$. The stream lines on midsurface in the VD and in the area of the leading edge are presented in the mode of non-incidence flow ($i = -2^\circ$), with a large positive incidence

angle ($i = +6°$) and with a large negative incidence angle ($i = -8°$).

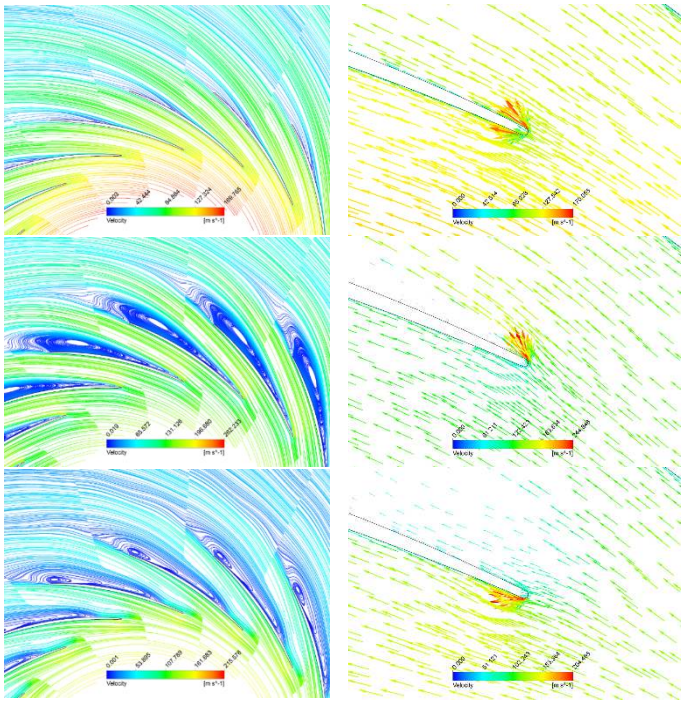

FIGURE 4: GAS FLOW STRUCTURE AT VD MID-SPAN AT DIFFERENT INCIDENCE ANGLES. TOP: $i = -2°$, MIDDLE: $i = -8°$ BOTTOM: $i = +6°$,

With a small negative incidence angle, the critical flow stream turns towards the curved surface where the gas pressure is less and forms a front critical point in the middle of the leading edge of the vane. This is a condition of non-incidence entry.

With a large negative incidence angle, the critical point is shifted towards the suction side. Flowing around the leading edge with a small radius of curvature, the gas accelerates at the beginning of the pressure side. With flow stagnating, a large separation zone is formed.

With a large positive incidence angle, the critical point is shifted towards the pressure side. Flowing around the leading edge with a small radius of curvature, the gas accelerates at the beginning of the suction side. But the separation of the flow is again formed on the pressure side. The formation of separation on the pressure side is characteristic of movement in curved channels.

Figure 5 shows the stream lines in two VD with the minimum of the researched relative height of the vanes $\bar{b}_3 = 0.025$ and different vane curvature angles $\Delta\alpha_v = 10°$ and $20°$. The number of vanes is 16 and 19 respectively, which corresponds to approximately the same density of the vane row $l/t = 1.854$ and 1.861.

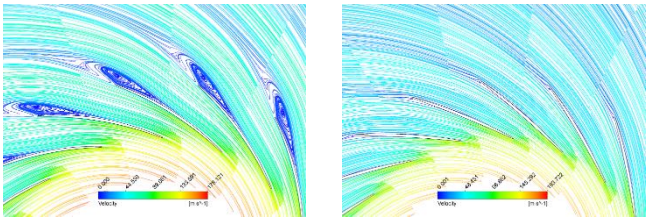

FIGURE 5: STREAM LINES AT VD MID-SPAN AT ZERO INCIDENCE ANGLE. $\bar{b}_3 = 0.025$. LEFT $\Delta\alpha_v = 10°$, RIGHT $\Delta\alpha_v = 20°$

Figure 6 shows similar data for two diffusers with the maximum of the researched relative vane height $\bar{b}_3 = 0.080$ and the same dimensions of the vane row.

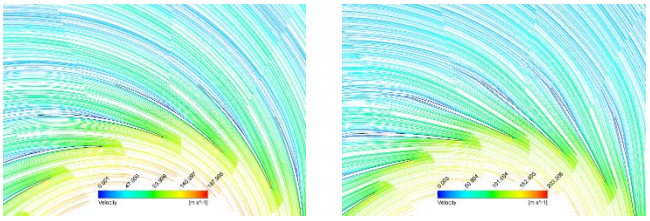

FIGURE 6: STREAM LINES AT VD MID-SPAN AT ZERO INCIDENCE ANGLE. $\bar{b}_3 = 0.080$ LEFT $\Delta\alpha_v = 10°$, RIGHT $\Delta\alpha_v = 20°$.

Flow separations occur in all four diffusers, in three cases – on a pressure side. For the variant in figure 6 on the right, a small gap appeared on the rear, suction side. A more intense separation zone occurs at a lower angle of curvature. It seemed logical that the separation should be more intense in channels that have a larger ratio $\frac{f_4}{f_3} = \frac{\sin\alpha_{v4}}{\sin\alpha_{v3}}\frac{D_4}{D_3}$, i.e. in diffusers with a large angle of curvature. But it turned out that the curvature of the pressure surface of the vane affects the separation stronger. At $\Delta\alpha_v = 20°$ the back surface of the vane is almost straight, and the radius of curvature of the front, convex surface is very large. This form of vanes is recommended in [8].

3.2 Analysis of the characteristics of vane diffusers with different relative widths and angles of vane curvature

Objects of research are vane diffusers with relative width $\bar{b}_3 = 0.025, 0.034, 0.045, 0.06, 0.08$. Diffusers with different relative widths at the same angles of curvature have the same elementary vane rows. The number of vanes was assumed such that the row density was close to the recommended one according to the results of the experimental research [17]:

- at $\Delta\alpha_v = 10°$ investigated number of vanes 16, 17, 18, $l/t = 1.85–2.09$;
- at $\Delta\alpha_v = 15°$ investigated number of vanes 18, 19, 20, $l/t = 1.91–2.12$;
- at $\Delta\alpha_v = 20°$ the investigated number of vanes 19, 20, 21, $l/t = 1.86–2.06$.

Diffuser width $\bar{b}_3 = 0.025$. The characteristics of efficiency, recovery coefficient and loss coefficient (above

family of curves, mean family of curves, below family of curves respectively in figures 7 - 11) are shown in figure 7.

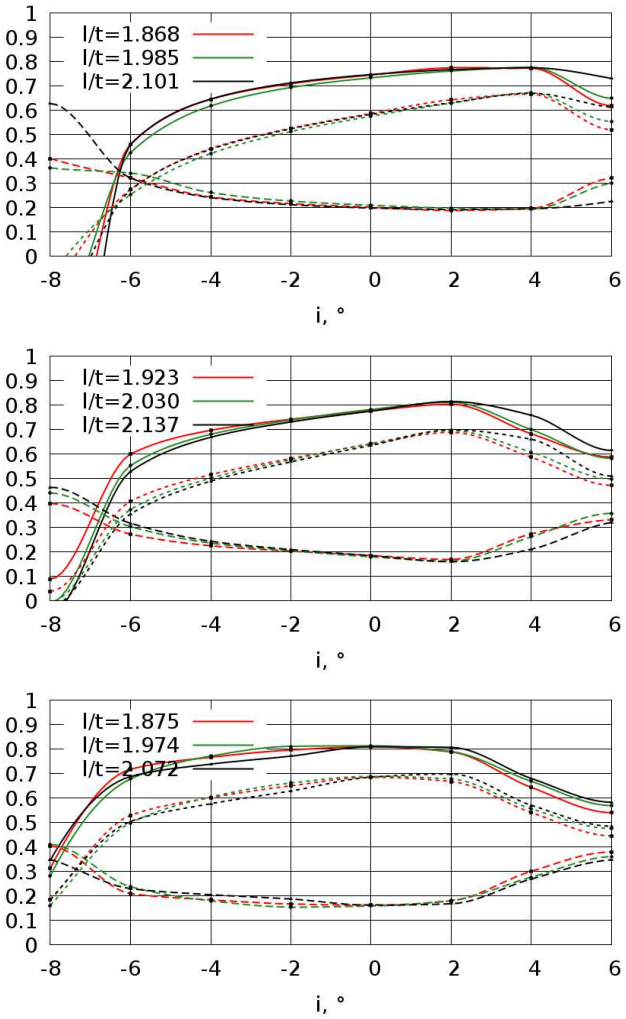

FIGURE 7: CHARACTERISTICS OF VD WITH $\bar{b}_3 = 0.025$, $\alpha_3 = 20°$. TOP $\Delta\alpha_v = 10°$, MIDDLE $\Delta\alpha_v = 15°$, BOTTOM $\Delta\alpha_v = 20°$

The number of vanes or the density of the row practically does not affect the characteristics at $\Delta\alpha_v = 10°$. At $\Delta\alpha_v = 15°$, the rarest row with $l/t = 1.923$ ($z = 16$) is less efficient. At $\Delta\alpha_v = 20°$ the maximum efficiency does not depend on the number of vanes. At $l/t = 1.875$ and 1.974, the diffuser is more effective at negative incidence angles. With more vanes ($l/t = 2.072$), the diffuser is more efficient at positive incidence angles, which is important for industrial compressors. The maximum efficiency of 0.816 and the recovery factor of 0.697 take place at an incidence angle $+2°$ at VD with $\Delta\alpha_v = 15°$, $z = 20$, $l/t = 2.12$.

Diffusers with the lowest curvature angle of 10° are inferior in efficiency and recovery coefficient and are not of practical interest. The VD boundary of effective operation is at $\Delta\alpha_v = 15°$ and 20° in case of incidence angle $-6°$. At this boundary the VD with the maximum angle of curvature is more effective. For industrial compressors more efficient operation of the VD in the design mode and modes with reduced flow, i.e. at positive incidence angles is more important. Here VD with $\Delta\alpha_v = 15°$ is better.

Diffuser width $\bar{b}_3 = 0.034$. The characteristics of efficiency, recovery coefficient and loss coefficient are shown in figure 8. The figure shows the densities of the vane rows corresponding to the numbers of vanes shown above.

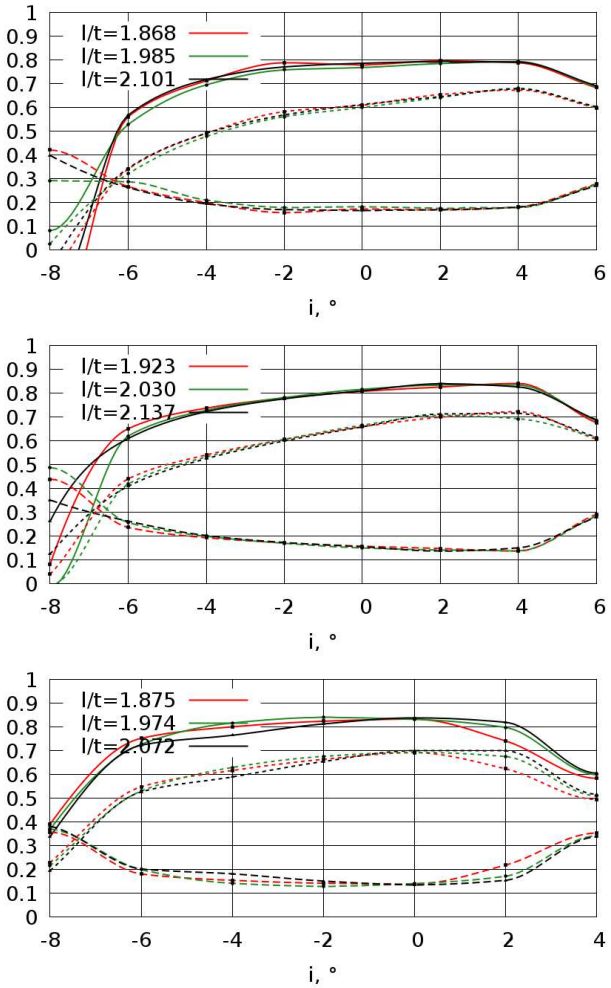

FIGURE 8: CHARACTERISTICS OF VD WITH $\bar{b}_3 = 0.034$, $\alpha_3 = 20°$. TOP $\Delta\alpha_v = 10°$, MIDDLE $\Delta\alpha_v = 15°$, BOTTOM $\Delta\alpha_v = 20°$

The character of the influence of density and angle of curvature is similar to VD with $\bar{b}_3 = 0.025$. The maximum efficiency of 0.84 and the recovery coefficient of 0.711 take place at an incidence angle $+2°$ at VD with $\Delta\alpha_v = 15°$, $z = 20$, $l/t = 2.12$ (the same elementary vane row is more effective at $\bar{b}_3 = 0.025$). With 18 vanes, $l/t = 1.91$, the maximum efficiency is 1.4% lower. But at high flow rates (negative incidence angles), this VD is more effective.

Diffusers with the lowest curvature angle of 10° are inferior in efficiency and recovery coefficient.

Diffuser width $\bar{b}_3 = 0.045$. The characteristics of efficiency, recovery coefficient and loss coefficient are shown in figure 9. The figure shows the densities of the vane rows corresponding to the numbers of vanes shown above.

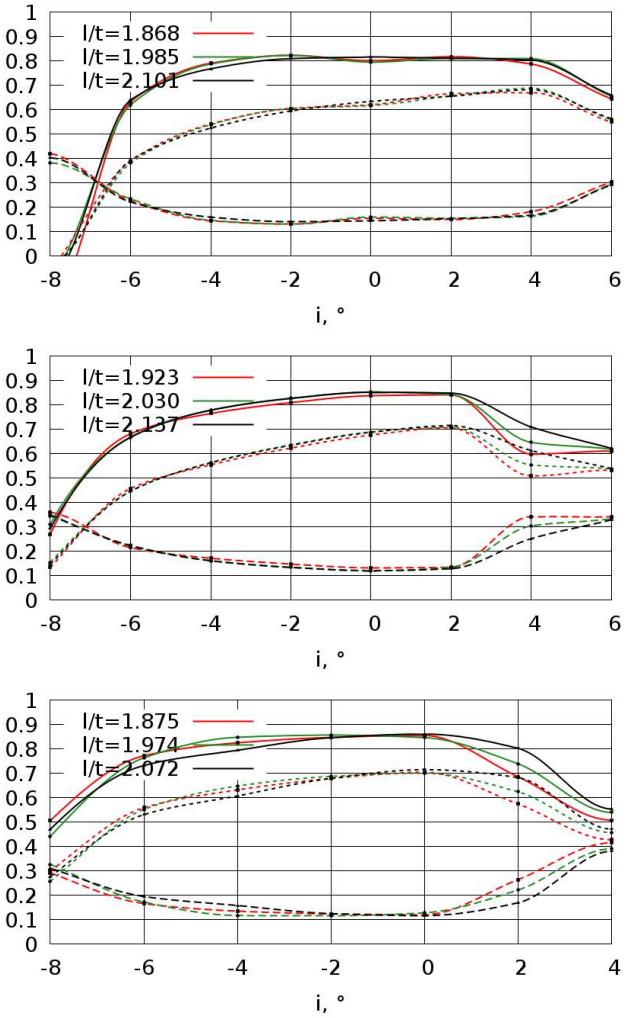

FIGURE 9: CHARACTERISTICS OF VD WITH $\bar{b}_3 = 0.045$, $\alpha_3 = 20°$. TOP $\Delta\alpha_v = 10°$, MIDDLE $\Delta\alpha_v = 15°$, BOTTOM $\Delta\alpha_v = 20°$

For VD with $\bar{b}_3 = 0.045$ rows with maximum angle of curvature of 20° are more suitable. Such vanes are shown above in the figure 9. The outlet angle of the VD is 40° despite the fact that the straight vane has an outlet angle of 44.46°. For VD with $\Delta\alpha_v = 20°$, $z = 21$, $l/t = 2.06$ the greatest efficiency is 0.861 and the rate recovery is 0.714—at zero incidence angle.

Diffusers with the lowest curvature angle of 10° are inferior in efficiency and recovery coefficient.

Diffuser width $\bar{b}_3 = 0.06$. The characteristics of efficiency, recovery coefficient and loss coefficient are shown in figure 10. The figure shows the densities of the vane rows corresponding to the numbers of vanes shown above.

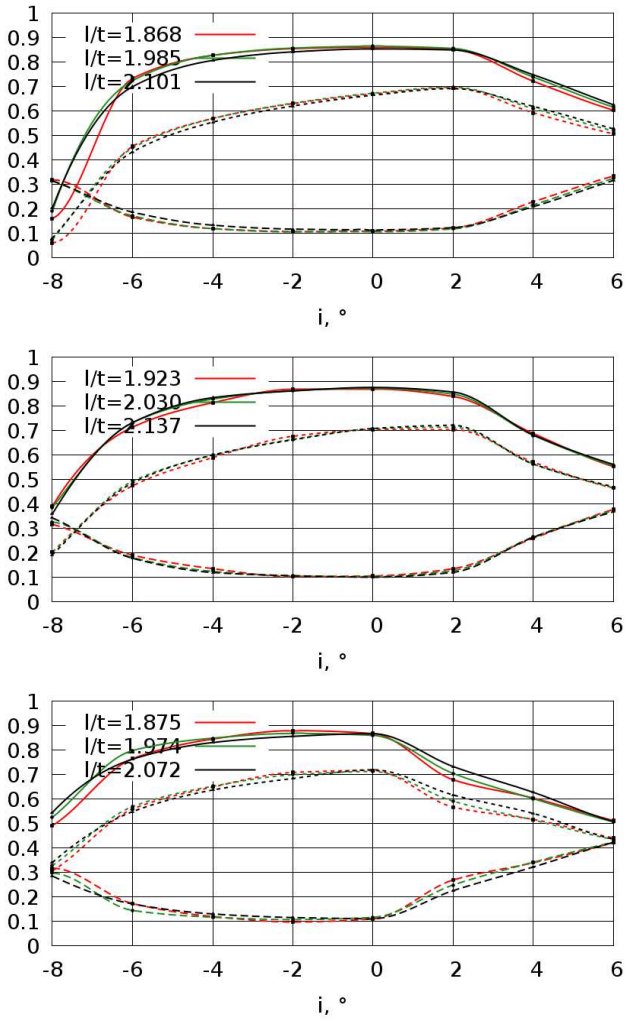

FIGURE 10: CHARACTERISTICS OF VD WITH $\bar{b}_3 = 0.06$, $\alpha_3 = 20°$. TOP $\Delta\alpha_v = 10°$, MIDDLE $\Delta\alpha_v = 15°$, BOTTOM $\Delta\alpha_v = 20°$

The highest efficiency is equal to 86.6% at an incidence angle of $-2°$ at VD with $\Delta\alpha_v = 15°$, $z = 20$, $l/t = 2.12$. It also has the highest recovery coefficient but at an incidence angle of $+2°$. Diffusers with a large angle of curvature have a lower coefficient of recovery. The maximum of this coefficient is achieved at zero incidence angle. This is a disadvantage for the vane diffuser of an industrial compressor which should work well at flow rates less than it was designed for.

Diffusers with the lowest curvature angle of 10° are inferior in efficiency and recovery coefficient.

Diffuser width $\bar{b}_3 = 0.08$. The characteristics of efficiency, recovery coefficient and loss coefficient are shown in figure 11. The figure shows the densities of the vane rows corresponding to the numbers of vanes shown above.

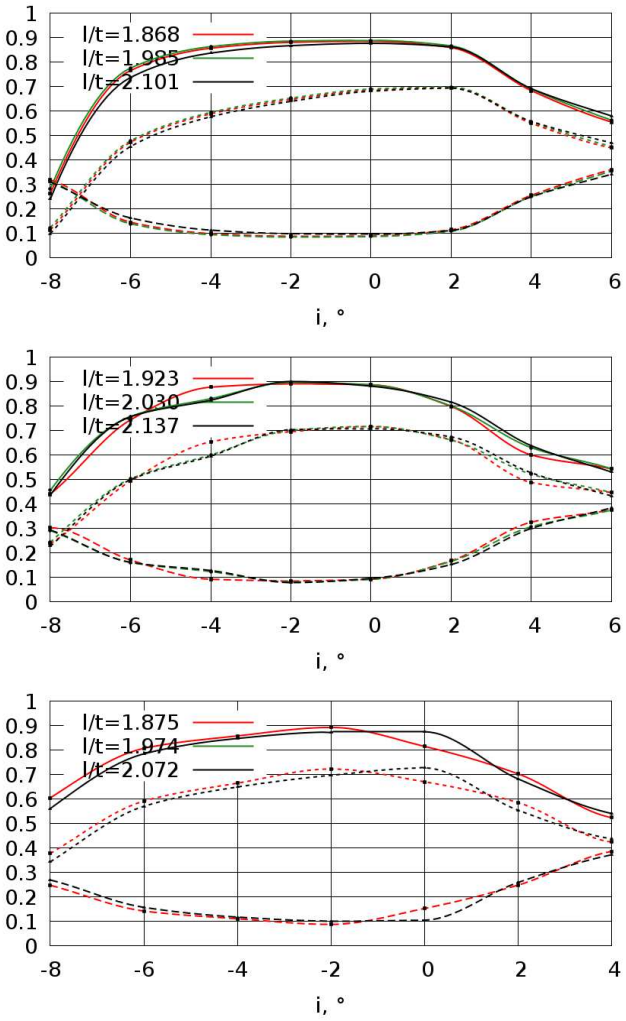

FIGURE 11: CHARACTERISTICS OF VD WITH $\bar{b}_3 = 0.08$, $\alpha_3 = 20°$. TOP $\Delta\alpha_v = 10°$, MIDDLE $\Delta\alpha_v = 15°$, BOTTOM $\Delta\alpha_v = 20°$

As with narrower diffusers, the angle of curvature $\Delta\alpha_v = 10°$ is not effective. Efficiency is equal to 89.2% and the coefficient recovery is equal to 0.697 in case of VD with $\Delta\alpha_v = 15°$, $l/t = 1.909$ are achieved with incidence angle of $-2°$. Efficiency is equal to 89.2% and the recovery coefficient is equal to 0.722 for VD with $\Delta\alpha_v = 20°$, $l/t = 1.851$ are achieved also with incidence angle of $-2°$. The greater recovery coefficient of this VD is an advantage. But when choosing a diffuser, it should be noted that the increase of $\Delta\alpha_v$ and decrease of l/t shift the characteristic towards negative incidence angles. With a slightly positive incidence angle a flow separation develops and the solution becomes unstable. We can observe poor convergence of iterative processes for high positive and negative values of incidence angle. This flow regime corresponds to surge limit in a stage and to maximum flow rate of a stage where operation is forbidden.

3.3 Features of the flow deviation angle in the vane row of the centrifugal stage diffuser

In [8] the formula by A. Howell for calculation of the flow deviation angle on a nominal mode in a blade row of the axial compressor is given:

$$\Delta B^* = m\Theta\sqrt{\frac{t}{B}}, \Theta = \beta_{bl2} - \beta_{bl2}, m = 0.23 \cdot 2\bar{B}_f^2 + 0.18 \quad (15)$$

where $\bar{B}_f$ is the distance from the leading edge to the maximum curvature arm of the profile related to the chord of the profile B.

The empirical formula (15) by structure completely corresponds to non-separable character of gas flow in a row:

– the greater the number of vanes the smaller the relative pitch t/B (less vane load) and the smaller the deviation angle;
– the greater the curvature of the vanes Θ the greater the load the greater the deviation angle;
– the greater the geometric parameter $\bar{B}_f$ the greater the load of the vanes is shifted to the row exit and the greater the deviation angle.

Typical dependencies of the deviation angle on the incidence angle are given on the example of VD with $\bar{b}_3 = 0.025, \Delta\alpha_v = 10°$, $\bar{b}_3 = 0.06, \Delta\alpha_v = 20°$, $\bar{b}_3 = 0.08, \Delta\alpha_v = 15°$ – figure 12.

Naturally, the deviation angle increases with the increase of $\Delta\alpha_v$: the more the load, the more the deviation. At a low load of slightly bent vanes at $\Delta\alpha_v = 10°$, the deviation angle value of $1-2$ degrees almost does not depend on the incidence angle in the working zone with a moderate flow separation in the VD with $\bar{b}_3 = 0.025 - 0.08$.

With a greater curvature the impact of the load is stronger. The load increases with positive incidence angles – the deviation angle increases too. But paradoxical is the influence of row density – the greater the relative pitch (less number of vanes) – the smaller the deviation angle. Obviously, we need to take into account the fact that the flow separation happens at all incidence angles. The picture of the stream lines in figure 13 offers this explanation.

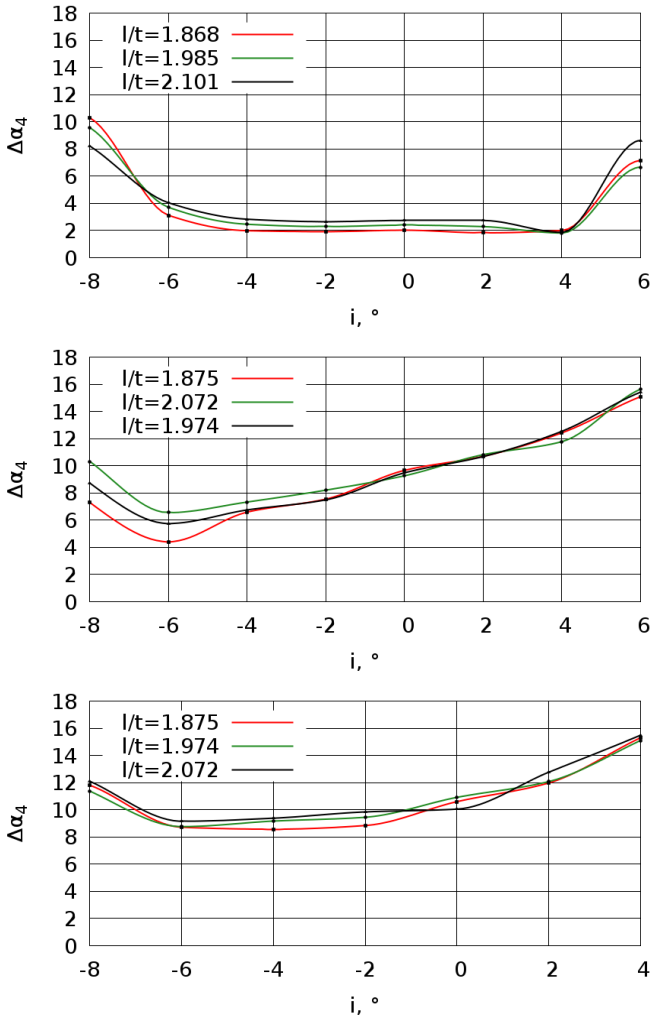

FIGURE 12: DEPENDENCE OF THE DEVIATION ANGLE FROM THE INCIDENCE ANGLE IN VD AT DIFFERENT ROW DENSITIES $l/t = 1.85 - 2.15$. $\bar{b}_3 = 0.025, \Delta\alpha_v = 10°$ TOP; $\bar{b}_3 = 0.06, \Delta\alpha_v = 20°$ MIDDLE; $\bar{b}_3 = 0.08, \Delta\alpha_v = 20°$ BOTTOM

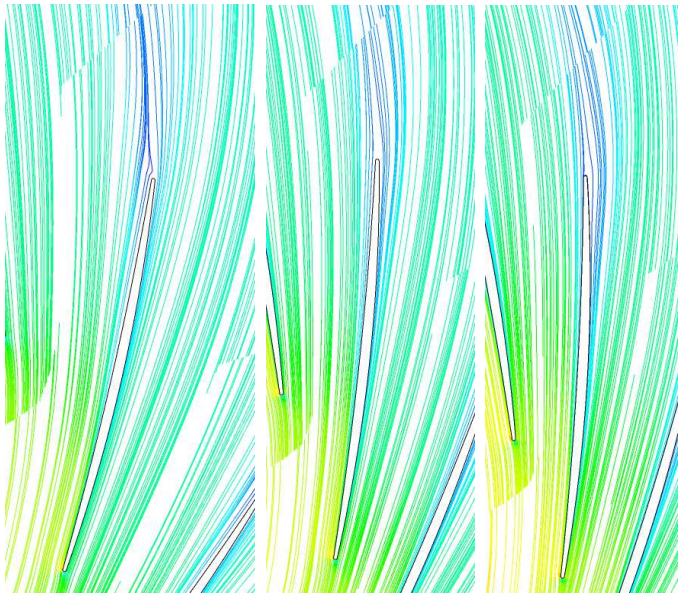

FIGURE 13: STREAM LINES ON MIDSURFACE OF THE VD. $\bar{b}_3 = 0.045, \alpha_3 = 20°, \Delta\alpha_v = 20°, i_3 = 0°$. LEFT $z = 15$, CENTER $z = 21$, RIGHT $z = 25$

At the number of vanes $z = 25$ separation occurs on the convex surface of the vanes. The direction of rotation of the vortices is counterclockwise, in the direction of the circumferential component of the velocity $c_{u4} > 0$. In the mixing process at the VD outlet the kinetic energy of the vortices increases the velocity circulation $\Gamma = 2\pi r c_u$. In this case, the deviation angle increases.

With the optimal number of vanes $z = 21$ the separation on the convex surface is minimal. The deviation angle does not exceed the one at $z = 25$.

With a further decrease of vane number, the separation passes to the suction side. The direction of rotation of the vortices is clockwise, against the positive direction $c_{u4} > 0$. In the mixing process at VD exit, the kinetic energy of the vortices reduces the velocity circulation and the deviation angle decreases.

The small influence of the load on the deviation angle in the row with slightly bent vanes is explained by the calculated load diagram $\Delta p = f(r)$, see figure 14.

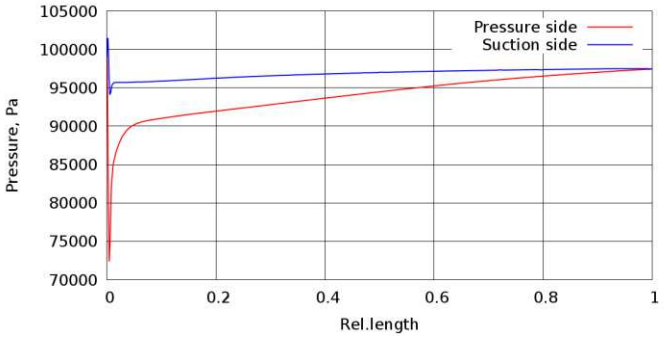

FIGURE 14: LOAD DIAGRAM OF THE DIFFUSER VANES. $\bar{b}_3 = 0.045, \alpha_3 = 20°, \Delta\alpha_v = 10°, i_3 = 0°, z = 10$

The pressure difference on the surfaces of the last third of the vanes is very small, namely the pressure difference causes the process of deviating the flow from the vanes direction. Close to zero values of the deviation angle in VD with small angles of curvature of the vanes are confirmed.

3.4 Discussion

CFD simulations of a series of vane diffusers in general gave quality results that coincide with the experiments and with the vane cascade theory.

Unexpected results:

- in the straight cascades more intense flow deflection leads to more intense separation zones. In the VD with a smaller angle of deflection in figure 5 flow separation is more intensive. Vane curvature is bigger and flow deceleration less intensive in case of smaller $\Delta\alpha_v$. The negative influence of the vane curvature prevails over the negative influence of the area ratio of the diffuser channel;
- in rows with almost straight vanes at a lower density the separation zone on the front surface decreases and even shifts to the very end of the suction side;
- in contrast to straight rows, the deviation angle in the VD circular rows tends to increase with increasing row density. The authors explain this with the complex nature of the interaction of the active part of the flow with the separation zones.

Obviously in the case of circular rows, density does not have such a strong influence on the characteristics. This corresponds to the results of experiments with model stages [21]. Figure 15 compares the characteristics of two variants of the model stage K101-1 of 20CE series with a vane diffuser with 16 and 8 vanes.

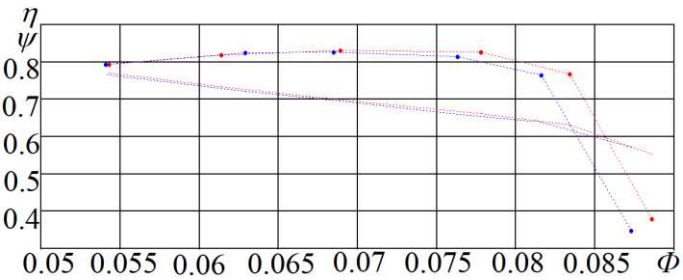

FIGURE 15: CHARACTERISTICS OF THE MODEL STAGE K101-1 VD, M_u=0.845. BLUE $z = 16$, $l/t = 2.24$. RED $z = 8$, $l/t = 1.12$.

The stage variant with a very low density $l/t = 1.12$ is not inferior to the variant with a more traditional row density in the left part of the characteristic. At $\Phi > 0.065$ VD with 8 vanes provides higher efficiency.

4. CONCLUSION

The main aim of the authors is to accumulate information about vane diffusers characteristics with different geometric parameters in order to create a mathematical model for an optimization design system. To create a mathematical model, it is enough to present the loss coefficient and the drag angle as the function of the incidence angle. Now the vane diffuser characteristics have not been researched in the entire range of geometric parameters. A computational research of the influence of similarity criteria is also required.

The authors believe that the presented results themselves may be of interest to aerodynamicists. The results obtained are generally consistent with the provisions of the vane cascade theory, but qualitatively differ from the test results of axial cascades of axial compressors. The authors attribute this to two circumstances:

- unlike axial diffuser cascades of axial compressors, in radial cascades of centrifugal compressors the deceleration is more sufficient, and flow separation occurs even with non-incidence inlet,

- unlike axial diffuser cascades of axial compressors, in radial cascades of centrifugal compressors, separation occurs on the pressure side of the vanes.

As a result, the influence of flow separation and cascade density on the drag angle is not the same as in axial diffuser cascades. The authors interpreted this as an unusual flow behavior. The computational research will continue until the accumulation of information sufficient to create a mathematical model. More information will make now unusual flow behavior familiar. The results of the research of diffusers with only one row inlet angle and one value of the outlet diameter are presented. The influence of similarity criteria has not been researched. This determines the direction of further work of the authors. As the results accumulate, efforts will be made to synthesize them.

DECLARATIONS

Funding: the research is partially funded by the Ministry of Science and Higher Education of the Russian Federation as part of World-class Research Center program (Contract No. 075-15-2020-934 dated 17.11.2020)

Financial interests: The authors declare they have no financial interests

Non-financial interests: none.

Conflicts of interest/Competing interests: the authors declare no conflict of interest

Availability of data and material: data is transparent

Code availability: not applicable

Authors' contributions: Conceptualization, A.Borovkov and V. Yadikin; methodology, Y.Galerkin and E. Petukhov; software, A.Drozdov; validation, V. Semenovskiy and O. Solovyeva; writing—review and editing, A.Rekstin and L.Marenina.

Ethics approval: not applicable

Consent to participate: not applicable

Consent for publication: yes

Acknowledgements: the calculations were performed using the supercomputer of the center "Polytechnic" SPbPU.

REFERENCES

[1] Borovkov, Alexey I. and Voinov, Igor B. and Galerkin, Yurii B. and Nikiforov, Alexandr G. and Nikitin, Mikhail A. Modeling of gas-dynamic characteristics on the example of a model stage of a centrifugal compressor. *Scientific and Technical Bulletin of SPbPU. Natural and engineering sciences*. Vol. 24 No. 2 (2018): pp. 44–57.

[2] Borovkov, Alexey I. and Voinov Igor B. and Rekstin, Alexey F. and Bakaev, Boris V. Modeling of characteristics of two-stage centrifugal gas compressor unit. *Scientific and Technical Bulletin of SPbPU. Natural and engineering sciences*. Vol. 25 No. 2 (2019): pp. 87–104.

[3] Borovkov, A.I. and Voinov, I.B. and Nikitin, M.A. and Galerkin, Yu. B. and Rekstin, A.F., Drozdov, A. A. Performance modeling for a single-stage pipeline centrifugal compressor. *Scientific and Technical Bulletin of SPbPU. Natural and engineering sciences*. Vol. 24 No. 3 (2018): pp. 153–175.

[4] Galerkin, Yu.B. and Drozdov, A.A. Optimization of stationary parts of highflow centrifugal compressor unit with axiradial impeller with CFD methods. *Scientific and Technical Bulletin of SPbPU. Natural and engineering sciences*. Vol. 4 No. 231 (2015): pp. 179-188.

[5] Galerkin, Yu.B. and Solovyova, O.A. Improvement of vaneless diffuser calculations based on CFD experiment. Part 1. *Compressor technology and pneumatics* No. 3 (2014): pp. 35-41.

[6] Galerkin, Yu.B., Solovyova, O.A. Improvement of vaneless diffuser calculations based on CFD experiment. Part 2. *Compressors and pneumatics* No. 4 (2014): pp. 15-21.

[7] Galerkin, Yu.B. Mathematical simulation of centrifugal compressor stages at department of compressor engineering of SPbSTU. *Proceedings of symposium*. Hannover, Germany, 1992

[8] Galerkin, Yu. B. *Turbocompressors*. LTD information and publishing center KHT. Moscow (2010)

[9] Galerkin, Yu.B., Rekstin, A.F., Soldatova, K.V., Drozdov, A.A., Popov, Yu.A. Development of compressor engineering scientific school of LPI-SPbPU, results of collaboration with compressor engineers. *Proceedings of 17th international scientific and technical conference*. Kazan. Russia, 2017

[10] Galerkin, Yu.B., Drozdov, A.A. New version of Universal modeling method for centrifugal compressors calculation. *Omsk Scientific and Technical Bulletin. Aerospace and power engineering series.* Vol. 3 No. 2 (2019): pp. 25-36.

[11] Idelchik, I. *Aerohydrodynamics of technological devices: (supply, branch and distribution of a stream on devices section).* Mechanical engineering. Moscow (1983)

[12] Lunev, A.T. Structure of design and testing method of natural gas compressor units flow paths. *Compressors and pneumatics.* No. 10 (2001): pp. 4-7.

[13] Lunev, A.T. Development of high efficient changeable flowparts of centrifugal compressor units. PhD Thesis. Kazan, 2005

[14] Marenina, L.N. CFD wind tunnel tests of centrifugal stage return channel vane cascades. *Compressors and pneumatics*. No. 3 (2016): pp. 27-35

[15] Rekstin A.F., Galerkin Yu.B., Petukhov E.P. CFD-calculation method for vane diffusers of a centrifugal compressor stage. IOP Conference Series: Materials Science and Engineering. 604. 012051, 2019

[16] Rekstin, A.F., Soldatova, K.V., Galerkin, Yu.B. The Verification of a Simplified Mathematical Model of the Centrifugal Compressor Stages. *Proceedings of Higher Educational Institutions*. Vol. 9 No. 702 (2018).

[17] Ris, V.F. *Centrifugal compressors machines*. Mechanical engineering. Leningrad (1981)

[18] Seleznev, K.P., Galerkin, Yu.B. *Centrifugal compressors*. Mechanical engineering. Leningrad (1982)

[19] Solovyova, O.A. Mathematical model for gasdynamic characteristics calculation and optimization of centrifugal compressor stages vaneless diffusers. PhD Thesis. Peter the Great St.Petersburg Polytechnic University, St.Petersburg, 2018

[20] Soldatova, K.V. Development of the new mathematical model of centrifugal compressor flow part and model stages database. PhD Thesis. St.Petersburg State Polytechnic University, St.Petersburg, 2017

[21] Galerkin, Yu.B. *Proceedings of SPbSTU compressor engineering scientific school*. SPbSTU publishing centre, St.Petersburg, 2010

[22] Khisameev, I.G., Maksimov, V.A., Batkis, G.S., Guselbaev, Y.Z. *Design and operation industrial centrifugal compressors*. Fan publishing. Kazan (2012)

[23] Babák, M. Effective computational procedure for high pressure ratio centrifugal compressor. *Proceedings of TechSoft Engineering & SVS FEM Konference ANSYS*. Berlin, Germany, 2009

[24] Galerkin, Yu.B., Danilov, K.A., Popova, E.Y. Universal Modelling for Centrifugal Compressors-Gas Dynamic Design and Optimization Consepts and Application. *Proceedings of Yokohama International Gas Turbine Congress*. Yokohama, Japan, 1995

[25] Galerkin, Yu.B., Soldatova, K.V. Universal modeling method application for development of centrifugal compressor model stages. *Proceedings of International Conference on Compressors and their Systems*. London, UK, 2013

[26] Galerkin, Yu.B., Soldatova, K.V., Drozdov, A.A. New version of the universal modelling for centrifugal compressor gas dynamic design. *Proceedings of Purdue Conference*. Purdue, USA, 2014

[27] Galerkin, Yu.B., Drozdov, A.A., Solovyeva, O.A. Vaneless diffuser for low flow rate centrifugal

compressor stage. *Proceedings of 13th European Conference on Turbomachinery Fluid dynamics & Thermodynamics. ETC2019-329*. Lausanne, Switzerland, April 8-12, 2019

[28] Japikse, D., Bitter, J. Effective two-zone modeling of diffusers and return channel systems for radial and mixed-flow pumps and compressors. *Proceedings of 11th International symposium on transport phenomena and dynamics of rotating machinery*. Honolulu, USA, February 26 – March 02, 2006

[29] Japikse, D., Dubitsky, O. Vaneless diffuser advanced model. *Proceedings of ASME Turbo Expo Conference*. Reno-Tahoe, USA, June 6 – 9, 2005

[30] Japikse, D. Agile engineering and the restructuring of modern design. *Proceedings of 40th Israel Annual Conference on Aerospace Science*. Tel-Aviv and Haifa, Israel, February 23 – 24, 2000

[31] Rekstin, A.F., Drozdov, A.A., Solovyova, O.A., Galerkin, Yu.B. Two mathematical models centrifugal compressor stage vaneless diffuser comparison. *Proceedings of Oil and Gas Engineering (OGE-2018)*. Omsk, Russia, 2018.

[32] Rekstin, A.F., Popova, Y., Ucehovscy, A. Centrifugal compressor stages efficiency analysis by means of the approximate algebraic equations. *Proceedings of Oil and Gas Engineering (OGE-2018)*. Omsk, Russia, 2018.

[33] Seleznev, K.P., Galerkin, Yu.B. Mathematical Modeling of Performance Characteristics and Optimization of Turbomachine Stages. *Proceedings of international gas turbine congress.* Tokyo, Japan, 1983

[34] Prasad, Vemu V. and Kumar, Lava M. and Reddy, Madhusudhan B. Centrifugal compressor fluid flow analysis using CFD. *Science Insights: An International Journal*. No. 1 (2011) pp. 6 - 10.

Figures

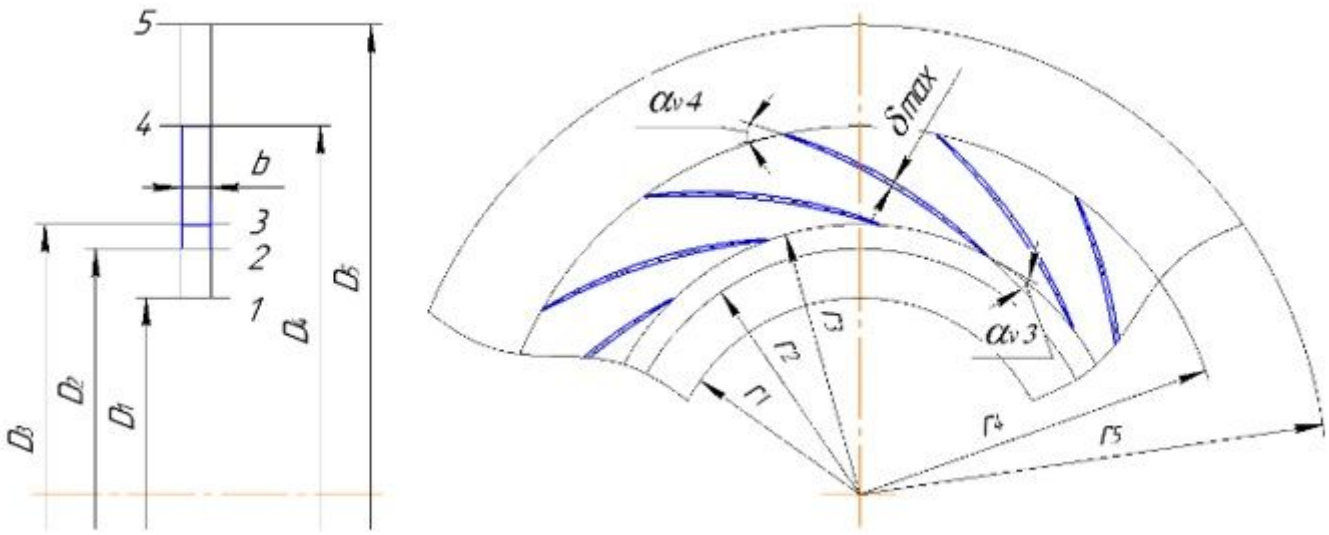

Figure 1

(see Manuscript file for figure legend)

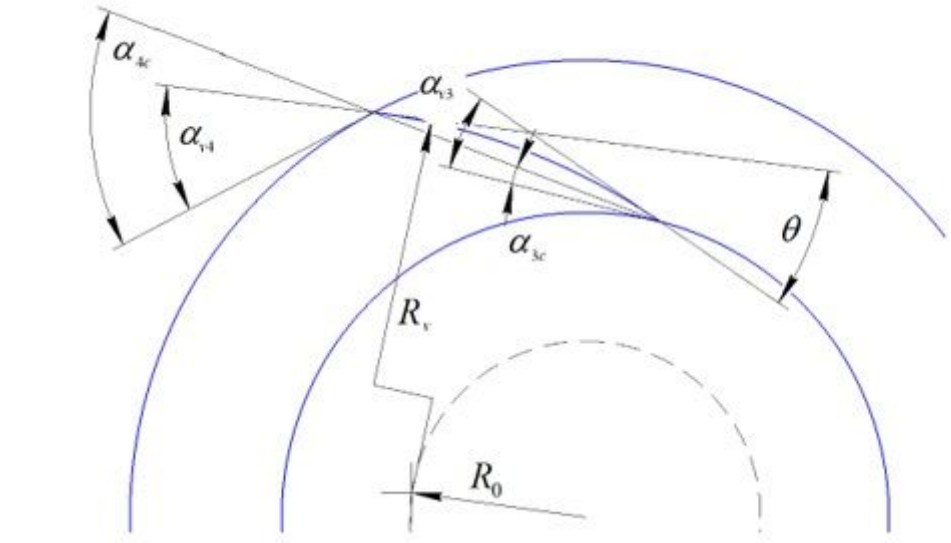

Figure 2

(see Manuscript file for figure legend)

Figure 3

(see Manuscript file for figure legend)

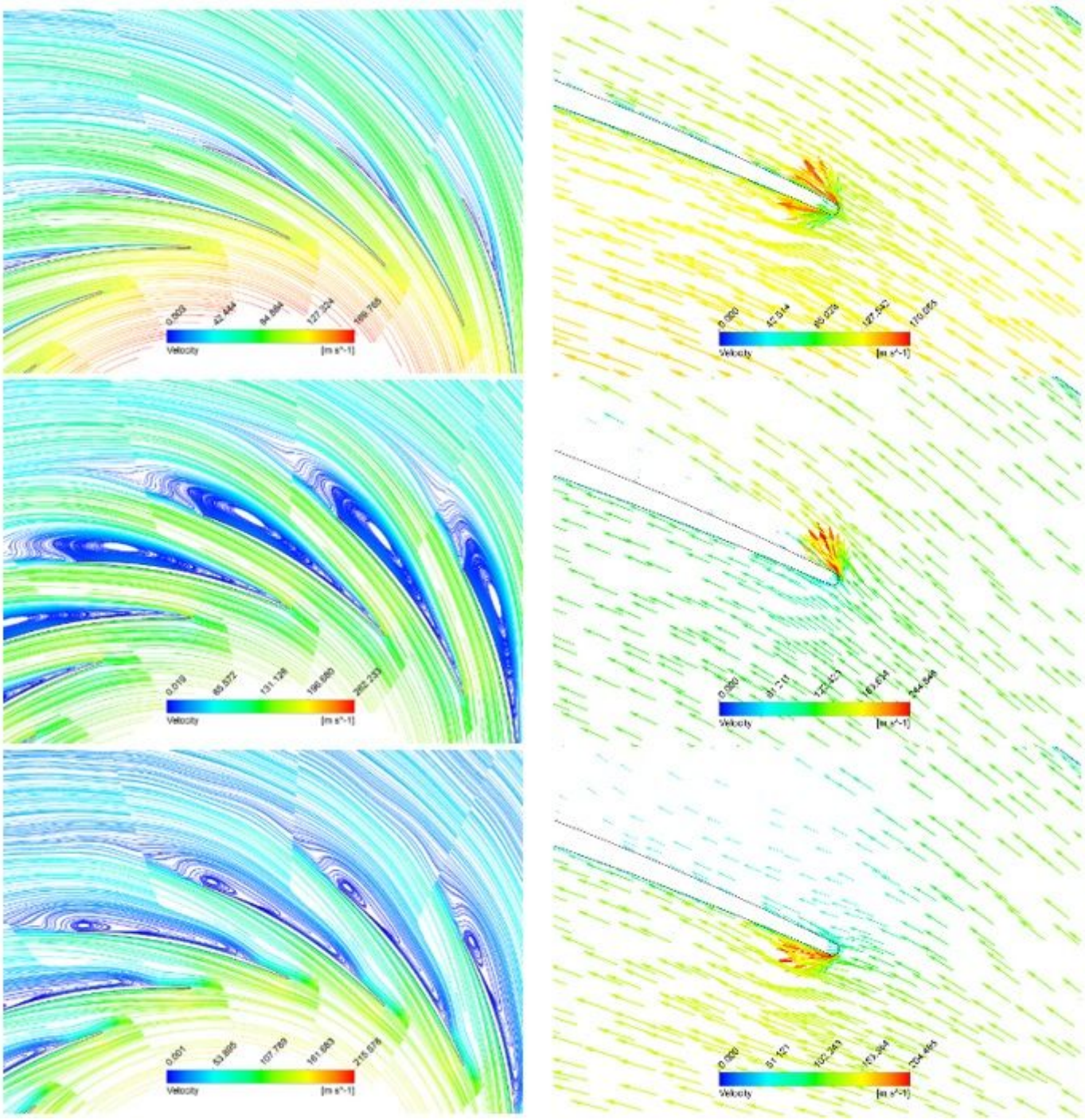

Figure 4

(see Manuscript file for figure legend)

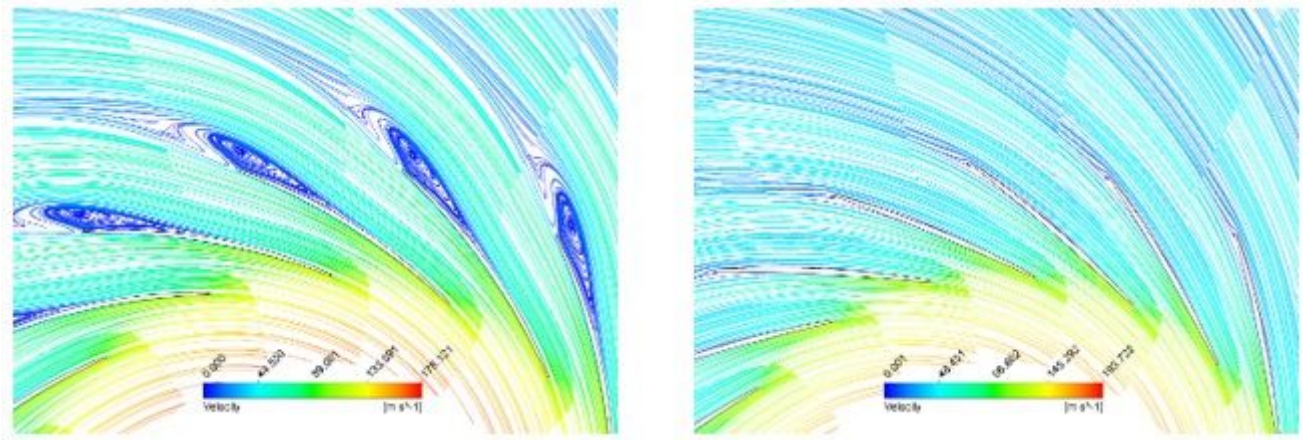

Figure 5

(see Manuscript file for figure legend)

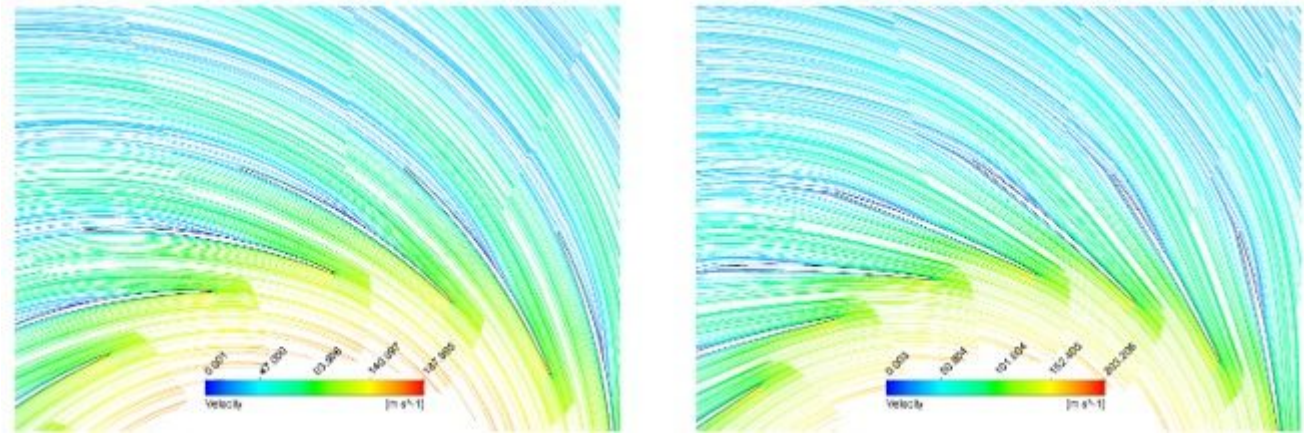

Figure 6

(see Manuscript file for figure legend)

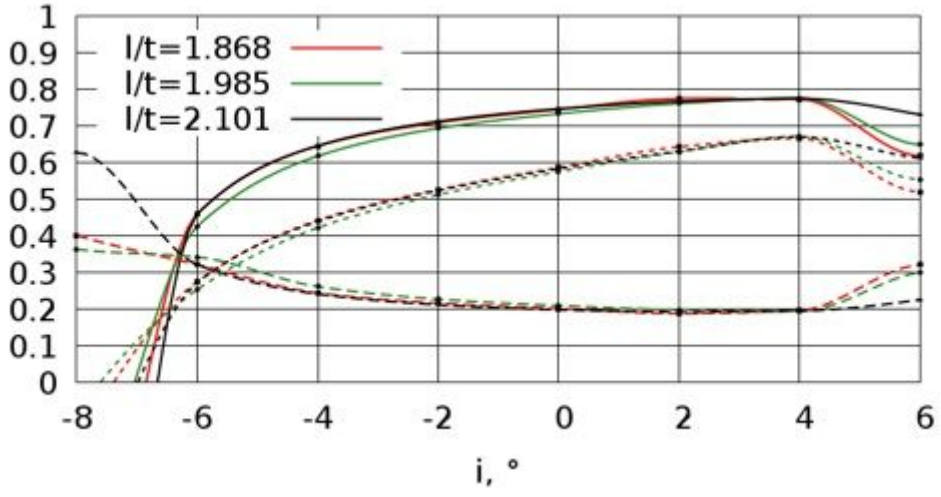

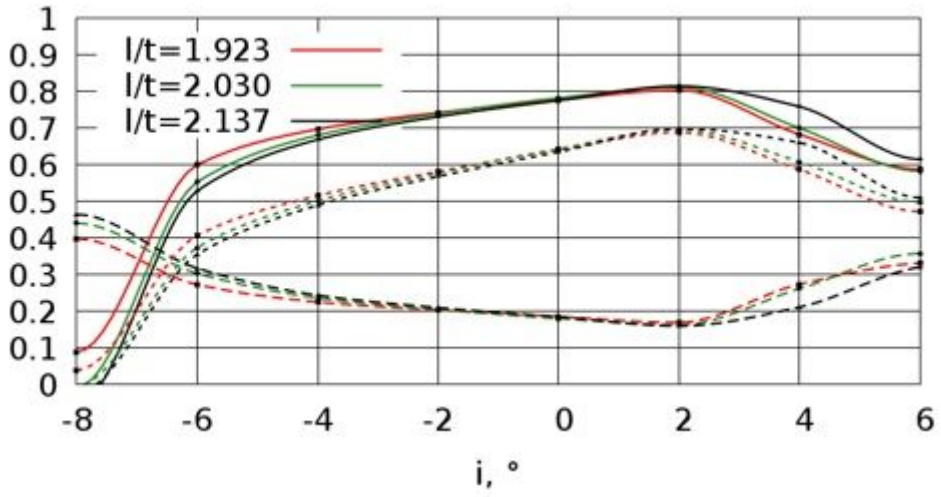

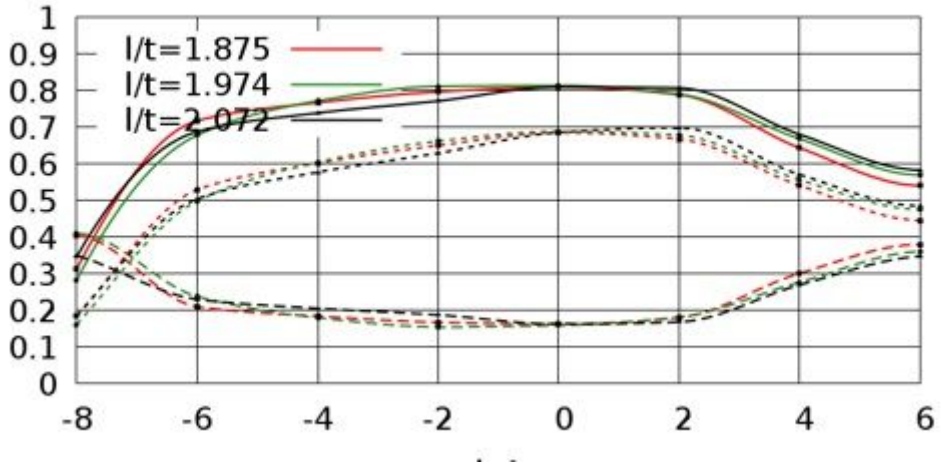

Figure 7

(see Manuscript file for figure legend)

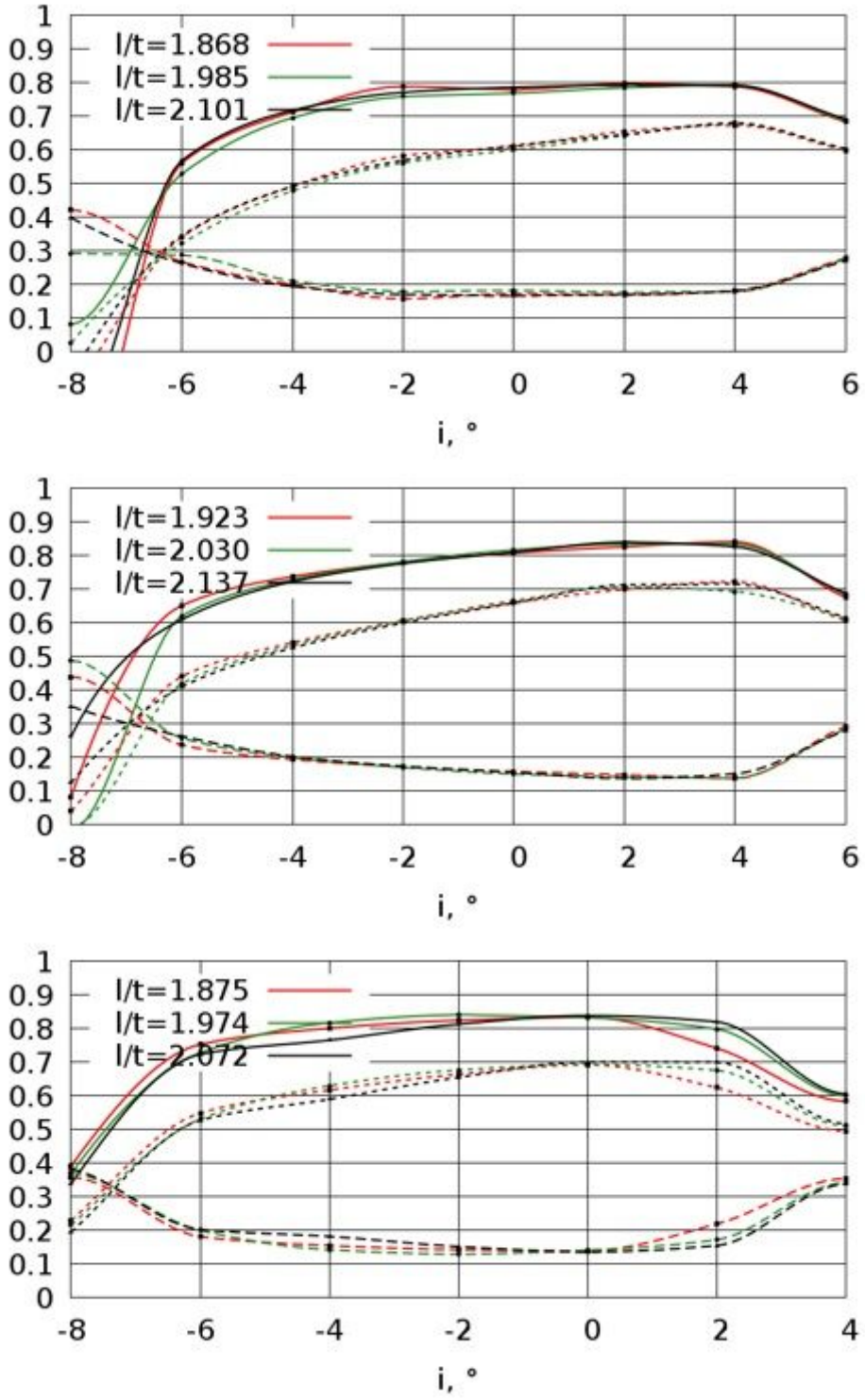

Figure 8

(see Manuscript file for figure legend)

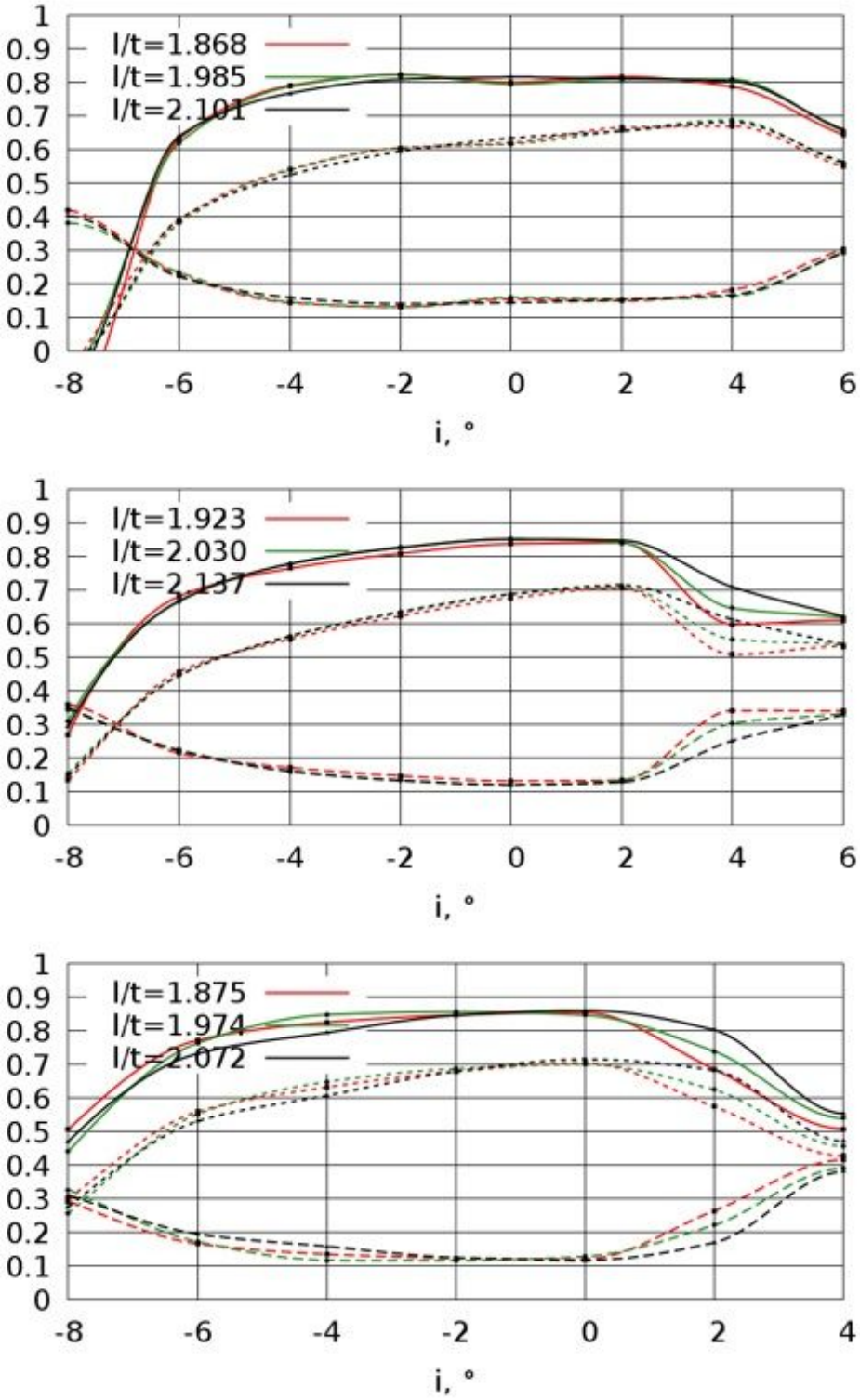

Figure 9

(see Manuscript file for figure legend)

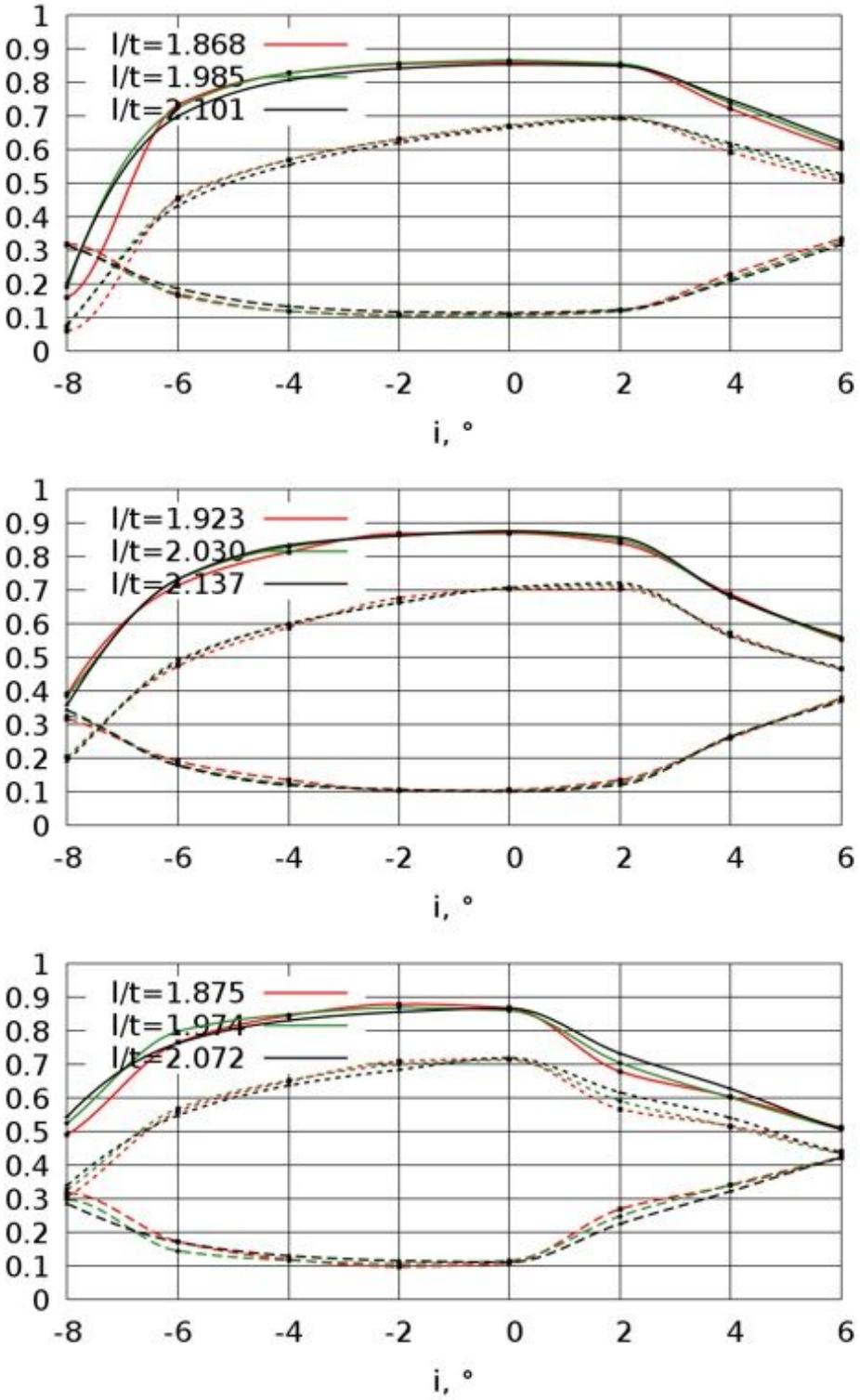

Figure 10

(see Manuscript file for figure legend)

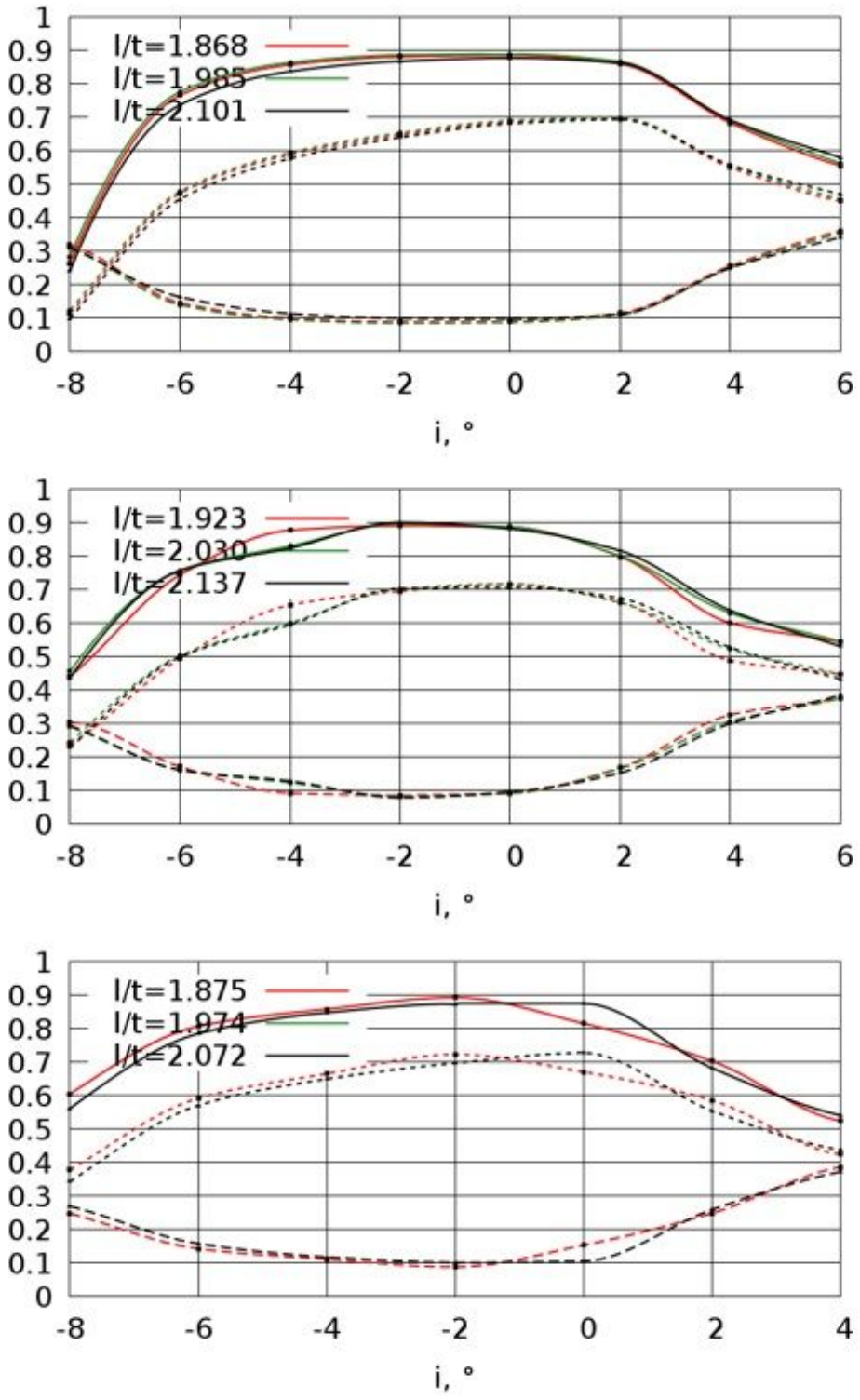

Figure 11

(see Manuscript file for figure legend)

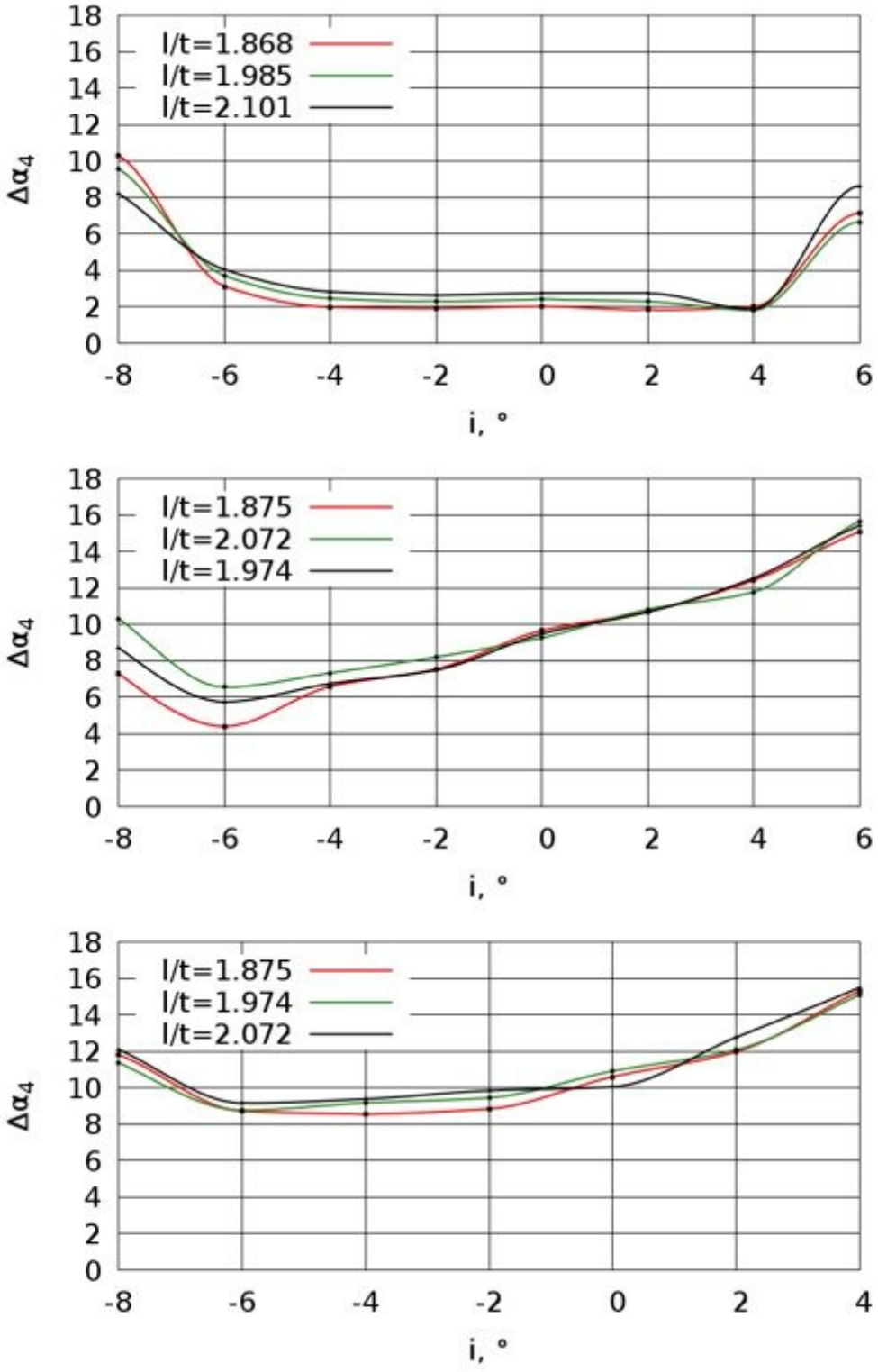

Figure 12

(see Manuscript file for figure legend)

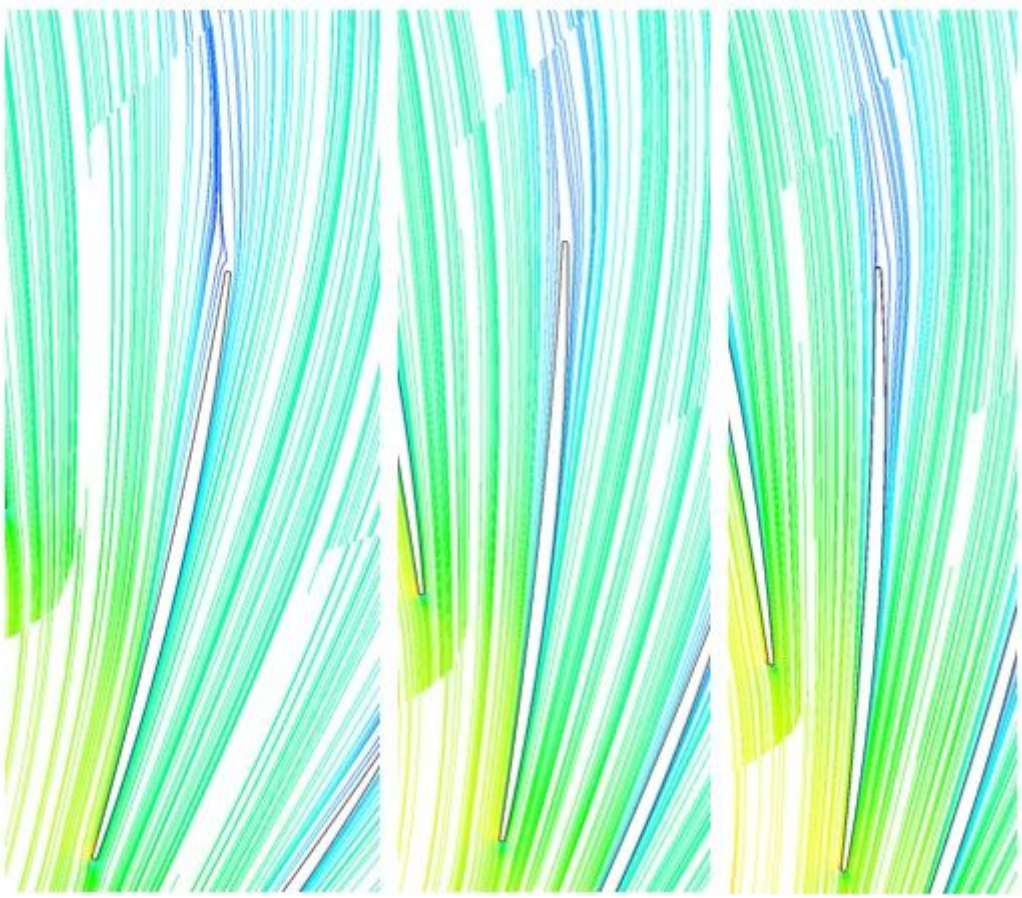

Figure 13

(see Manuscript file for figure legend)

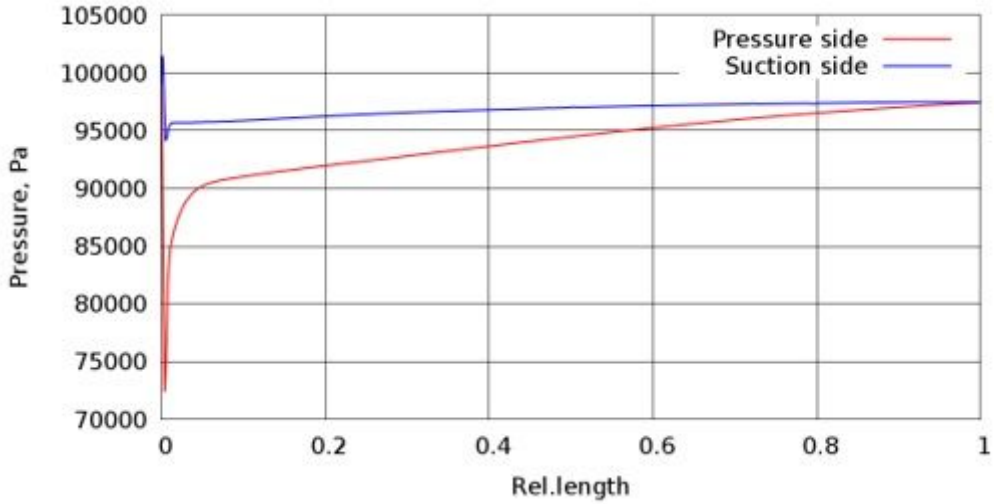

Figure 14

(see Manuscript file for figure legend)